NEURAL REGENERATION RESEARCH
November 2017, Volume 12, Issue 11
www.nrronline.org

RESEARCH ARTICLE

Neural progenitor cells but not astrocytes respond distally to thoracic spinal cord injury in rat models

Tara Nguyen, Yilin Mao, Theresa Sutherland, Catherine Anne Gorrie*
School of Life Sciences, Faculty of Science, University of Technology Sydney, New South Wales, Australia

How to cite this article: *Nguyen T, Mao Y, Sutherland T, Gorrie CA (2017) Neural progenitor cells but not astrocytes respond distally to thoracic spinal cord injury in rat models. Neural Regen Res 12(11):1885-1894.*
Funding: *This study was supported by UTS Faculty of Science Early Career Research Grant to CAG.*

Abstract

Traumatic spinal cord injury (SCI) is a detrimental condition that causes loss of sensory and motor function in an individual. Many complex secondary injury cascades occur after SCI and they offer great potential for therapeutic targeting. In this study, we investigated the response of endogenous neural progenitor cells, astrocytes, and microglia to a localized thoracic SCI throughout the neuroaxis. Twenty-five adult female Sprague-Dawley rats underwent mild-contusion thoracic SCI (n = 9), sham surgery (n = 8), or no surgery (n = 8). Spinal cord and brain tissues were fixed and cut at six regions of the neuroaxis. Immunohistochemistry showed increased reactivity of neural progenitor cell marker nestin in the central canal at all levels of the spinal cord. Increased reactivity of astrocyte-specific marker glial fibrillary acidic protein was found only at the lesion epicenter. The number of activated microglia was significantly increased at the lesion site, and activated microglia extended to the lumbar enlargement. Phagocytic microglia and macrophages were significantly increased only at the lesion site. There were no changes in nestin, glial fibrillary acidic protein, microglia and macrophage response in the third ventricle of rats subjected to mild-contusion thoracic SCI compared to the sham surgery or no surgery. These findings indicate that neural progenitor cells, astrocytes and microglia respond differently to a localized SCI, presumably due to differences in inflammatory signaling. These different cellular responses may have implications in the way that neural progenitor cells can be manipulated for neuroregeneration after SCI. This needs to be further investigated.

Key Words: *nerve regeneration; contusion; spinal cord; neuroinflammatory; ependymal cell; glial fibrillary acidic protein; microglia; nestin; neuroaxis; tanycyte; third ventricle; trauma; neural regeneration*

***Correspondence to:**
Catherine Anne Gorrie, Ph.D., Catherine.gorrie@uts.edu.au.

orcid:
0000-0001-5934-2492 (Catherine Anne Gorrie)

doi: *10.4103/1673-5374.219051*

Accepted: *2017-09-22*

Introduction

Acute spinal cord injury (SCI) is characterized by hemorrhage, and the release of glutamate, reactive oxygen species, and inflammatory cells (Liu et al., 1999; Fleming et al., 2006). This creates a toxic microenvironment for neurons in the area surrounding the lesion epicenter. During chronic SCI, scar-forming reactive astrocytes express high levels of glial fibrillary acidic protein (GFAP) at the lesion area in the ever-changing microenvironment (Eng and Ghirnikar, 1994). This creates an impenetrable barrier for viable neurons and axons to recover (Fitch and Silver, 2008). Furthermore, there is an influx in exogenous macrophages at the lesion site as well as activation of microglia into a phagocytic phenotype (Fitch and Silver, 2008; Neumann et al., 2009). In a normal spinal cord, non-activated microglia exhibit ramified, long and thin processes. However, during an insult, microglia become activated and go through morphological changes such as shorter and thicker processes as well as amoeboid-like appearance (Ayoub and Salm, 2003). Activated microglia and reactive astrocytes both contribute to the neuroinflammatory response of the SCI (Streit et al., 2004). However, completely removing the glial and immune response can be detrimental to the injured spinal cord since reactive astrocytes, activated microglia and macrophages can release cytokines that promote tissue repair and axonal recovery (Fleming et al., 2006; do Carmo Cunha et al., 2007; Karimi-Abdolrezaee and Billakanti, 2012).

Neural stem cells exist in the dentate gyrus of the hippocampus and subventricular zone of the lateral ventricles of the human brain (Eriksson et al., 1998; Taupin and Gage, 2002). It has now been established that neural progenitor cells (NPCs) also exist in the ependymal regions of the human spinal cord and in different regions of the brain such as the third ventricle (Ming and Song, 2005; Xu et al., 2005; Meletis et al., 2008; Migaud et al., 2010). During non-pathological conditions, ependymal cells proliferate slowly (Blasko et al., 2012) but after SCI, ependymal cells undergo proliferation and differentiation and up-regulate an intermediate protein called nestin (Shibuya et al., 2002; Meletis et al., 2008; Cizkova et al., 2009; Hamilton et al., 2009; Barnabe-Heider et al., 2010; Foret et al., 2010; Mao et al., 2016a). It may be possible that the manipulation of these NPCs and modulation of the microenvironment during the early stages of a SCI might promote neuronal differentiation and functional recovery.

Although mechanical trauma to a spinal cord may be localized, the cellular response can be quite widespread. We have found that there is an extensive activation of nestin positive cells throughout the human spinal cord in response to traumatic central nervous system (CNS) injury (Cawsey et al., 2015). In cases of a brain impact, or a high cervical SCI, cells as far away as the lumbar spinal cord reacted by expressing nestin. The nestin positive cells in the spinal cord exhibited long basal processes that extended from the central canal to the parenchyma (Rafols and Goshgarian, 1985). Morphologically, these were very similar to nestin positive cells lining the

third ventricle, which have reported to have neuroendocrine properties (Rodriguez et al., 2005; Xu et al., 2005). We were interested to see the caudal and rostral extent of the cellular response to a localized SCI. Therefore, in this study, we investigated the response of NPCs, astrocytes, microglia and macrophages at different levels of the neuroaxis in response to a vertebral T_{10} contusion injury in a rat model.

Materials and Methods

Animals

Twenty-five adult Sprague-Dawley female rats weighing 250–300 g were obtained from the Animal Resource Center (Perth, WA, Australia). Rats were housed in groups of 4 in large cages with *ad libitum* food and water with a 12-hour dark light cycle except immediately following injury and during the post-operative care period when they were housed individually. All animals were provided with environmental enrichment as part of the standard housing conditions. Animals were randomly assigned to one of three groups: normal (n = 8), sham surgery (n = 8) and mild contusion SCI (SCI; n = 9). The least number of animals in each group was provided for statistical significance. Female rats were used in this study for consistency according to previous studies (Mao et al., 2016a; Sutherland et al., 2017). We did not control for hormonal fluctuations within the cohort although females have been reported to recover better than males overall (Chan et al., 2013). All surgical procedures were conducted strictly under the guidelines described by the National Health and Medical Research Council code of conduct for animals and with the approval of the institutional Animal Care and Ethics Committee (UTS ACEC13-0069).

Surgical procedure

The full protocol of the surgical procedure was prepared according to a previous study (Gorrie et al., 2010). A mild contusion SCI was performed at vertebral level T_{10} in the SCI group. Rats in the sham surgery group underwent all aspects of the surgery except for contusion thoracic injury. Rats were anesthetized using a combination of 4% isoflurane (Veterinary Companies of Australia, Blacktown, NSW, Australia) and 1 L/min oxygen in an induction chamber and maintained at 2% isoflurane. Cephalothin sodium (DBL^{TM}, Pfizer, NSW, Australia; 33 mg/kg, subcutaneous (s.c.)), Buprenorphine hydrochloride – Temgesic (Reckitt Benchkiser Healthcare, Berkshire, UK; 0.03 mg/kg, s.c.) and Hartman's replacement solution (AHB2323, Baxter, Old Toongabbie, NSW, Australia; 0.015 mL/g, s.c.) were given prior to surgery. The area for incision was shaved and sterilized with betadine (Betadine, QLD, Australia). Rats were placed on a heat mat to maintain a rectal temperature of 37°C. A 2 cm incision was made at the midline of the thoracic region of the back. The T_{10} vertebra was exposed by blunt dissection of the connective tissue and muscle. T_{10} laminectomy was performed to expose the spinal cord before the rat was subjected to a mild contusion injury using the New York University Multicenter Animal SCI Study (MASCIS) Impactor (Basso et al., 1996) (National Institute of Health, NY, USA). SCI was induced by dropping a 10 g weight from 6.25 mm height with an impact head diameter of 2.5 mm. Parameters of the SCI including the spinal compression (mm), impact velocity (m/s) and impact time were recorded using the New York University MASCIS impactor software. The compression rate was calculated as the ratio of cord compression depth over time to ensure each SCI was consistent for each rat (Basso et al., 1996). The wound was closed in layers using an absorbable monocryl suture (Y496G, Johnson and Johnson, New Jersey, USA). Post-operative care included the administration of Cephalothin sodium (DBL^{TM}, Pfizer; 33 mg/kg, s.c.), Buprenorphine hydrochloride – Temgesic (Reckitt Benchkiser Healthcare; 0.03 mg/kg, s.c.), and Hartman's replacement solution (AHB2323, Baxter; 0.015 mL/g, s.c.) and manual expression of the bladder twice daily for 3 days. Manual expression of the bladder continued until normal voiding responses return.

Animal euthanasia and histological tissue preparation

At 24 hours post-injury, rats were euthanized using Lethabarb euthanasia injection (Virbac, Milperra, NSW, Australia; 0.001 mL/g, i.p.). Animals then underwent cardiac perfusion with cold saline followed by 4% paraformaldehyde (P6148, Sigma-Aldrich, St Louis, MO, USA). Brain and spinal cords were dissected out and post-fixed in 4% paraformaldehyde before cryoprotection in 30% sucrose solution. All tissue from each group was processed blindly except the tissue that had an obvious injury in the thoracic region. The macroscopic appearance of the injured cord showed hemorrhage and bruising (figure not shown). The injury extended approximately 2.25 mm away from the point of impact (epicenter) creating an oval-shaped lesion site. Coronal sections of the spinal cord including the cervical enlargement, three regions of the injury site at the thoracic segment and the lumbar enlargement were cut (15 μm thick) using a cryostat (CM1950, Leica Biosystems, VIC, Australia). One region of the brain at the level of the third ventricle was identified using Paxinos Rat Brain Atlas (Paxinos G., 1996). Coronal sections of the brains were cut (15 μm thick) using a cryostat. One section from each level of the neuroaxis was routinely stained with Mayer's hematoxylin (FNNII008, Fronine, Riverstone, NSW, Australia) and 1% alcoholic eosin (II016, Fronine, Riverstone, NSW, Australia) to assist in lesion identification and morphology observation.

Immunohistochemistry

Co-labeling of nestin and GFAP was performed to determine the immunoreactivity of NPCs and astrocytes respectively. All slides were immersed in 0.1 M phosphate buffer with saline (pH 7.4) with 0.1% (v/v) Tween 20 (PBST) for 10 minutes before a blocking agent of 5% normal goat serum (NGS) (G9023, Sigma-Aldrich, St. Louis, MO, USA) was applied for 30 minutes. Primary antibodies that were used for NPCs and astrocytes are mouse anti-nestin antibody (Abcam, Cambridge, UK; 1:200) and polyclonal rabbit anti-GFAP antibody (Dako, Glostrup, Denmark; 1:1,000). Double labeling of rabbit anti-IBA1 antibody (Abcam; 1:500) for microglia, and mouse anti-ED1 antibody (Serotec, Puchheim, Germany; 1:500) for macrophages was performed. Antibodies were diluted in phosphate buffer with saline (PBS) with 0.05% NGS and applied onto each slide before being incubated overnight at 4°C. Slides were then rinsed in PBST before a cocktail of AlexaFluor-488 anti-rabbit antibody (Invitrogen, Carlsbad, CA, USA;

1:200) and AlexaFluor-568 anti-mouse antibody (Invitrogen; 1:200) was applied onto slides treated with anti-nestin and anti-GFAP antibodies. AlexaFluor-568 anti-rabbit antibody (Invitrogen; 1:200) and AlexaFluor-488 anti-mouse antibody (Invitrogen; 1:200) were applied onto slides treated with anti-IBA1 and anti-ED1 antibodies. All slides were incubated for 2 hours at room temperature. After another rinse in PBST, a counterstain of Hoechst solution (33342, Invitrogen; 1:5,000) was applied for 10 minutes to stain the nuclei. Slides were rinsed with PBST once more before cover-slipping using an mounting medium (S3023, Dako, Glostrup, Denmark). Negative controls had the primary antibody omitted and brain sections contained internal positive controls.

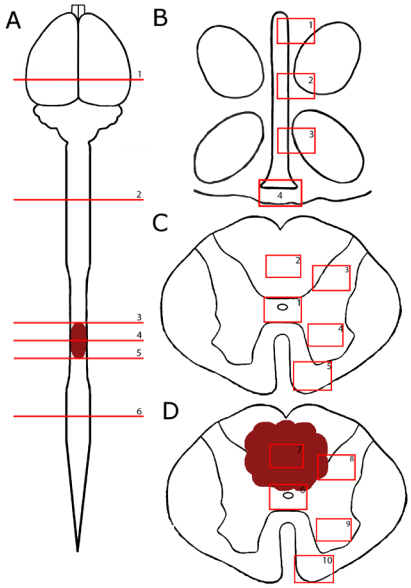

Figure 1 A schematic of different regions of the neuroaxis being investigated in thoracic spinal cord injury rats.
(A) The levels of the neuroaxis being investigated include: (1) the third ventricle, (2) cervical enlargement, (3) thoracic region 2.25 mm rostral to the epicenter, (4) thoracic region at the epicenter, (5) thoracic region 2.25 mm caudal to the epicenter and (6) lumbar enlargement. (B) Regions of the third ventricle include: (1) alpha region, (2) dorsal region, (3) ventral region, and (4) median eminence. Areas of the (C) normal and (D) injured spinal cord being investigated include (1, 6) central canal, (2) posterior median septum, (3) dorsal grey matter, (4, 9) ventral grey matter, (5, 10) ventral white matter, (7) lesion center and (8) lesion edge in spinal cord injury only.

Image analysis

High power images of nestin, GFAP, microglia and macrophage immunohistochemistry were taken using the cellSens controller and manager program on the Olympus BX-51 Upright Fluorescence Microscope Phase (Olympus, Toyko, Japan). Six sections of the neuroaxis that were investigated which included the third ventricle of the brain, cervical enlargement, thoracic segment (rostral, central and caudal to the epicenter) and the lumbar enlargement of the spinal cord as shown in **Figure 1A**. Regions of interest being investigated at the third ventricle are the alpha region, dorsal region, ventral region, and the median eminence (**Figure 1B**). Regions of interest being investigated in the injured spinal cord included the central canal, lesion center, lesion edge, ventral grey matter, and ventral white matter (**Figure 1D**). An equivalent area was chosen to compare the lesion center and lesion edge in the injured group. This area included the posterior median septum (lesion center) and dorsal grey matter (lesion edge) as shown in **Figure 1C** & **D**. The lesion center and lesion edge were determined from the hematoxylin and eosin stained sections, as the area with necrotic cells, hemorrhage and cellular debris.

Nestin and GFAP immunohistochemistry of each section was quantified using the mean gray scale value of each region of interest after the section had been black balanced to normalize any variance in background staining intensity between sections.

IBA1 and ED1 double-labeled sections were analyzed by manual cell counts of each area of the neuroaxis. This was not stereotaxic counts of each segment of the neuroaxis. Four subsets of microglia and macrophages were identified and determined by double-labeling and morphological appearances: $IBA^+/ED1^-$ ramified microglia which have thin and long processes with a small cell soma (**Figure 2A**), $IBA^+/ED1^-$ activated microglia which have either shorter processes or have an amoeboid-like appearance (**Figure 2B**), $IBA^+/ED1^+$ phagocytic microglia/macrophages which have an amoeboid appearance (**Figure 2C**), and $IBA^-/ED1^+$ exogenous macrophages which have an amoeboid appearance (**Figure 2D**).

Statistical analysis

All data presented are shown as the mean ± SD in each experimental group. Occasional sections were excluded in the

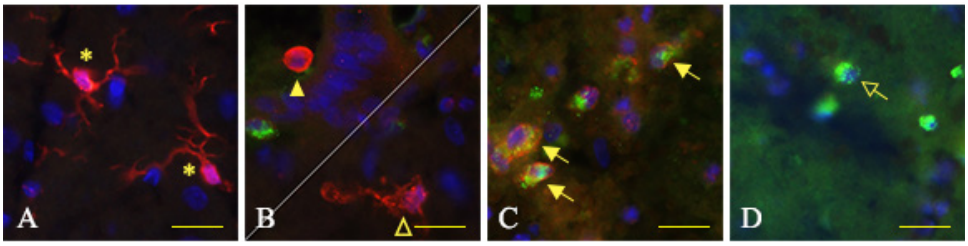

Figure 2 Immunohistochemical images of the four subsets of microglia/macrophages being investigated in thoracic spinal cord injury rats.
(A) $IBA1^+/ED1^-$ ramified microglia: long and thin processes extending to the parenchyma with a small cell soma (asterisk). (B) $IBA1^+/ED1^-$ activated microglia: exhibit two morphological appearances; short and thicker processes with a large cell soma (arrow head) or amoeboid-like appearance (open arrow head). (C) $IBA1^+/ED1^+$ activated microglia/macrophage: amoeboid-like appearance with very few, if any, processes (arrow). (D) $IBA1^-/ED1^+$ macrophages: amoeboid appearance with a large cell soma (open arrow). Scale bars: 10 μm.

analysis because of disruptive tissue due to the injury and this is reflected in the statistical analysis for quantification. For quantification of nestin and GFAP immunohistochemistry, images were converted to grayscale using ImageJ software (National Institutes of Health, NY, USA) and the mean gray scale value was calculated. A combination of one-way analysis of variance (ANOVA) and Bonferroni *post-hoc* test was used for statistical analysis of the mean gray scale value of nestin and GFAP. For IBA1 and ED1 statistical analysis, a combination of two-way ANOVA and Bonferroni *post-hoc* test was used. All statistical analyses were done using Graphpad Prism software version 6 (Graphpad software Incorporated, San Diego, CA, USA). A P value of < 0.05 was considered to be statistically significant.

Results

Surgical procedures

All surgical procedures were completed without any unexpected adverse events. The mean compression rate for the SCI group was 0.291 ± 0.027 ms^2. All rats recovered from surgery well and showed signs of impaired hind limb locomotor function consistent with the injury. None of the control rats showed any evidence of injury or impaired locomotor function.

Nestin positive cells throughout the neuroaxis after injury

Baseline nestin staining in the normal and sham surgery groups was seen in the ependymal layer of the third ventricle (**Figure 3A, G** & **M**). Occasional nestin positive cells were also seen in endothelial cells (Mokry et al., 2008) and quiescent ependymal cells (Lendahl et al., 1990) in the spinal cord (**Figure 3B–F, H–L**). The highest amount of nestin staining was seen in the median eminence, followed by the ventral and dorsal regions of the third ventricle. However, there was no significant difference in nestin staining between the SCI group and the normal and sham surgery groups (**Figure 4A**). Nestin staining was increased at the central canal of all spinal cord levels after thoracic SCI (**Figure 3N–R**). Nestin positive cells had long basal processes that extended into the parenchyma of the spinal cord. It was difficult to distinguish whether the nestin positive cells were located entirely in the ependymal layer or in the subependymal layer so we did not attempt to separate the two locations.

In all levels of the spinal cord, nestin reactivity increased in the ependymal cells of the central canal but not at the lesion center, lesion edge, ventral grey matter or ventral white matter (**Figure 4B–F**). Nestin staining intensity was significantly increased in the injured cords at the central canal in both normal and sham-operated cords in the cervical enlargement (ANOVA, F(2,22) = 16.87, P < 0.0001; **Figure 4B**), rostral to the thoracic epicenter (ANOVA, F(2,22) = 6.169, P < 0.0075; **Figure 4C**), at the epicenter (ANOVA, F(2,19) = 19.37, P < 0.0001; **Figure 4D**), caudal to the epicenter (ANOVA, F(2,21) = 9.347, P < 0.0012; **Figure 4E**) and in the lumbar enlargement (ANOVA, F(2,22) = 11.59, P < 0.0004; **Figure 4F**).

GFAP positive cells throughout the neuroaxis after injury

In the spinal cord, GFAP staining was seen in single astrocytes scattered throughout the white and grey matter. After injury there can be an increase in astrocyte number as well as a change in morphology with individual astrocytes producing thicker processes and having a more ramified appearance (Sun and Jakobs, 2012). Together, this results in an increase in GFAP staining intensity. Baseline GFAP immunoreactivity at the third ventricle (**Figure 5A, G** & **M**) existed in both the ependymal cells and their processes and in the surrounding astrocytes in the parenchyma. No significant difference existed at the third ventricle, cervical enlargement, thoracic segment rostral to the epicenter and the lumbar enlargement in the injury group compared to the normal and sham groups (**Figure 5M–O, Q** & **R**).

GFAP staining intensity appears to be increased at the lesion edge of the epicenter (**Figure 5P**). At the thoracic epicenter, there was an increase in GFAP staining intensity at the central canal (ANOVA, $F(2,15) = 13.62$, P < 0.0004), the lesion edge (ANOVA, $F(2,22) = 38.29$, P < 0.0001) and the ventral grey matter (ANOVA, $F(2,17) = 4.503$, P < 0.0001) (**Figure 4J**) in the injured group compared to the normal and sham groups. Caudal to the thoracic epicenter, GFAP was significantly decreased at the lesion center (ANOVA, $F(2,17) = 4.503$, P < 0.05, **Figure 4K**) in the injured group compared to the normal group. No significant differences were found in the regions of the third ventricle, cervical, and lumbar segments (**Figure 4G, H** & **L**) or at the thoracic segment rostral to the epicenter (**Figure 4I**). In all 3 groups, the ventral white matter showed the highest level of GFAP immunoreactivity throughout the spinal cord but there were no significant difference between groups.

Macrophages and microglia throughout the neuroaxis after injury

In the CNS, there is a normal distribution of ramified microglia in the third ventricle (**Figure 6A**) and spinal cord (**Figure 6B–F**). In the SCI group, there was a morphological change in IBA1$^+$/ED1$^-$ cells, switching from long processes to shorter processes and a larger cell soma (**Figure 6R**). At the epicenter of the injury site, IBA1$^+$/ED1$^+$ and IBA1$^-$/ED1$^+$ cells were present in high numbers with amoeboid-like appearance (**Figure 6P**). There was a significant decrease in IBA1$^+$/ED1$^-$ ramified microglia at the thoracic segment rostral to the epicenter (ANOVA, $F(2,87) = 126.6$, P < 0.0001; **Figure 7C**), at the epicenter (ANOVA, $F(2,90) = 169.9$, P < 0.0001; **Figure 7D**), caudal to the epicenter (ANOVA, $F(2,88) = 126.6$, P < 0.0001; **Figure 7E**) and in the lumber segment (ANOVA, $F(2,82) = 101.5$, P < 0.0001; **Figure 7F**). No significant difference was found at the third ventricle and cervical segment (**Figure 7A** & **B**). In contrast, activated microglia (IBA1$^+$/ED1$^+$) were significantly increased at the cervical segment (ANOVA, $F(2,101) = 8.151$, P < 0.0001; **Figure 7H**), the thoracic segment rostral to the epicenter (ANOVA, $F(2,93) = 151.6$, P < 0.0001; **Figure 7I**), at the epicenter (ANOVA, $F(2,97) = 52.11$, P < 0.0001; **Figure 7J**), caudal to the epicenter (ANOVA, $F(2,97) = 82.27$, P < 0.0001; **Figure 7K**) and in the lumber segment (ANOVA, $F(2,94) = 90.83$, P < 0.0001; **Figure 7L**). No significant difference was found at the third ventricle in the brain (**Figure 7G**).

During SCI, the innate immune system involves the activation of microglia into phagocytic phenotypes and the recruitment of macrophages (Streit et al., 2004; Greenhalgh and David, 2014; Zhou et al., 2014). From our results, there was a significant increase in IBA1$^+$/ED1$^+$ cells at the thoracic segment rostral to the epicenter (ANOVA, $F(2,95) = 46.54$, P < 0.0001; **Figure 7O**),

at the epicenter (ANOVA, $F(2,97) = 68.7$, $P < 0.0001$; **Figure 7P**), and caudal to the epicenter (ANOVA, $F(2,84) = 37.23$, $P < 0.0001$; **Figure 7Q**). No significant difference was found beyond the lesion site (**Figure 7M, N** & **R**). Exogenous macrophages ($IBA1^-/ED1^+$) were significantly increased only at the thoracic segment rostral to the epicenter (ANOVA, $F(2,94) = 30.75$, $P < 0.0001$; **Figure 7U**), at the epicenter (ANOVA, $F(2,94) = 85.16$, $P < 0.0001$; **Figure 7V**), and caudal to the epicenter (ANOVA, $F(2,94) = 56.32$, $P < 0.0001$; **Figure 7W**). No significant difference was found beyond the lesion site (**Figure 7S**, **T** & **X**).

Discussion

This study has shown that nestin immunoreactivity was increased 24 hours post-injury throughout the spinal cord but not in the third ventricle in response to a mild thoracic SCI. Activated microglia was also found in the lumbar segment of the injured spinal cord. In contrast, GFAP immunoreactivity and macrophage cell counts were found only at the thoracic regions indicating a localized response.

NPCs have been identified in the ependymal layer lining the central canal in the spinal cord (Meletis et al., 2008; Hamilton et al., 2009). They have been shown to proliferate and differentiate into astrocytes and oligodendrocytes following SCI (Ke et al., 2006; Meletis et al., 2008; Cizkova et al., 2009; Hamilton et al., 2009; Barnabe-Heider et al., 2010; Foret et al., 2010). However, these cells can be induced towards a neuronal lineage in culture using mitogens such as fibroblast growth factor-2 and epidermal growth factor (Tureyen et al., 2005), and when cells are subjected to gene manipulation *in vivo* (Schwindt et al., 2009). Moreover, Sox11, a neural development transcription factor, was introduced into mice using lentiviral vectors and has been shown to activate endogenous NPCs after SCI, promoting locomotor activity (Guo et al., 2014). This suggests that NPC manipulation may have the potential to assist in repair and recovery following SCI. This may occur by inducing cell replacement, stimulating differentiation into neurons or changing the microenvironment of the lesion site by reducing astrocyte differentiation, but these potential therapeutic strategies remain to be determined. In a previous study (Cawsey et al., 2015), we found increased nestin positive ependymal cells at all levels of the human spinal cord following CNS injury, indicating a widespread activation of NPCs. This has also previously been shown in a rat model of compression SCI (Takahashi et al., 2003). The nestin positive cells seen in the ventricular systems of the brain closely resemble tanycytes that have been previously described (Weiss et al., 1996; Prieto et al., 2000; Martens et al., 2002). In this location, there is extensive literature reporting the neuroendocrine function of these cells and their involvement with transmitting signal from the cerebrospinal fluid (CSF) to the portal veins and the hypothalamus (Rodriguez et al., 2005; Haan et al., 2013; Goodman and Hajihosseini, 2015). In the spinal cord, the basal processes of the nestin positive ependymal cells also extended to blood vessels and it is possible that they have a similar function in CSF signal transmission. However, these nestin positive cells in the spinal cord have also been shown to exhibit neural progenitor-like qualities where they can be isolated, proliferated and differentiated in culture (Shihabuddin, 2008; Decimo et al., 2011). The fact that nestin positive cells are responding along the length of the spinal cord suggests that they are reacting to signals within the CSF rather than local cues in the tissue itself. Studies have shown that cytokines like interleukin (IL)-6, growth regulated oncogene (equivalent to IL-8 in rodents), IL-8 and monocyte chemoattractant protein-1 are increased in the CSF of human patients (Kwon et al., 2010) and spinal cord tissue in rodent models (Stammers et al., 2012). These factors may well be upregulating the expression of nestin in the ependyma. We do not know whether this response may be part of a generalized immune response, or whether it relates to a signal for increased cell production in response to injury.

Astrocyte proliferation and migration following SCI can be explained as part of the repair process of the CNS. Our results have shown that astrocytes begin to activate in response to the injury at 24 hours at the lesion site. Overtime, activated astrocytes will continue to chemically and physically change at the lesion site and become incorporated into a glial scar which acts in part to seal off the injury site from pathogens and in part to attempt to repair the injury by laying down additional extracellular matrix such as chondroitin sulphate proteoglycan (Morgenstern et al., 2002; Gaudet and Popovich, 2014; Ohtake et al., 2016). The GFAP response at this early time point seems to indicate that astrocytes are only responding locally to the injury, yet GFAP levels in CSF are higher in more severely injured individuals 24 hours post SCI in humans (Kwon et al., 2017). GFAP levels were also increased in blood samples from severe SCI patients (Ahadi et al., 2015). Gwak and Hulsebosch have reported that there was GFAP immunoreactivity in the lumbar segment after a T_{13} SCI, however, the lumbar segments investigated were in closer proximity to the injury site hence showing a remote astrocytic response beyond the lesion site (Gwak and Hulsebosch, 2009).

This study was a relatively simple investigation of tissue sections using immunohistochemical methods. We have examined three spinal levels and one brain region at one early post-injury time point and have demonstrated a robust change in nestin expression in the spinal cord ependymal cells lining the central canal. It would be of great interest to compare the surface receptors on the nestin positive cells between the spinal cord and the third ventricle to identify sub-populations of cells. In addition, it will be critical to establish a direct link between inflammatory factors in CSF and a response by the ependymal cells, and this would best be conducted through *in vitro* experiments. The cross-talk between the endogenous nervous system cells and the inflammatory response is extensive and may have a significant effect on the behavior of cells in the secondary injury progression. Moreover, it would be interesting to investigate NPC reactivity throughout the neuroaxis within different age groups since nestin reactivity at the spinal cord has also been observed in both infants and juvenile rats at 24 hours post-SCI (Sutherland et al., 2017).

The innate immune response during a SCI results in an influx of macrophages flooding into the injury site. Activated microglia are also present at the injury site where they migrate towards the lesion, and release cytokines like IL-1α, IL-1β, IL-6, TNF-α and leukemia inhibitory factor that contribute to neuroinflammation (Pineau and Lacroix, 2007; Mortazavi et al., 2015). We have shown that microglia activation extended to the lumbar segment of the spinal cord during injury and exogenous macrophages were significantly increased at the lesion site. The

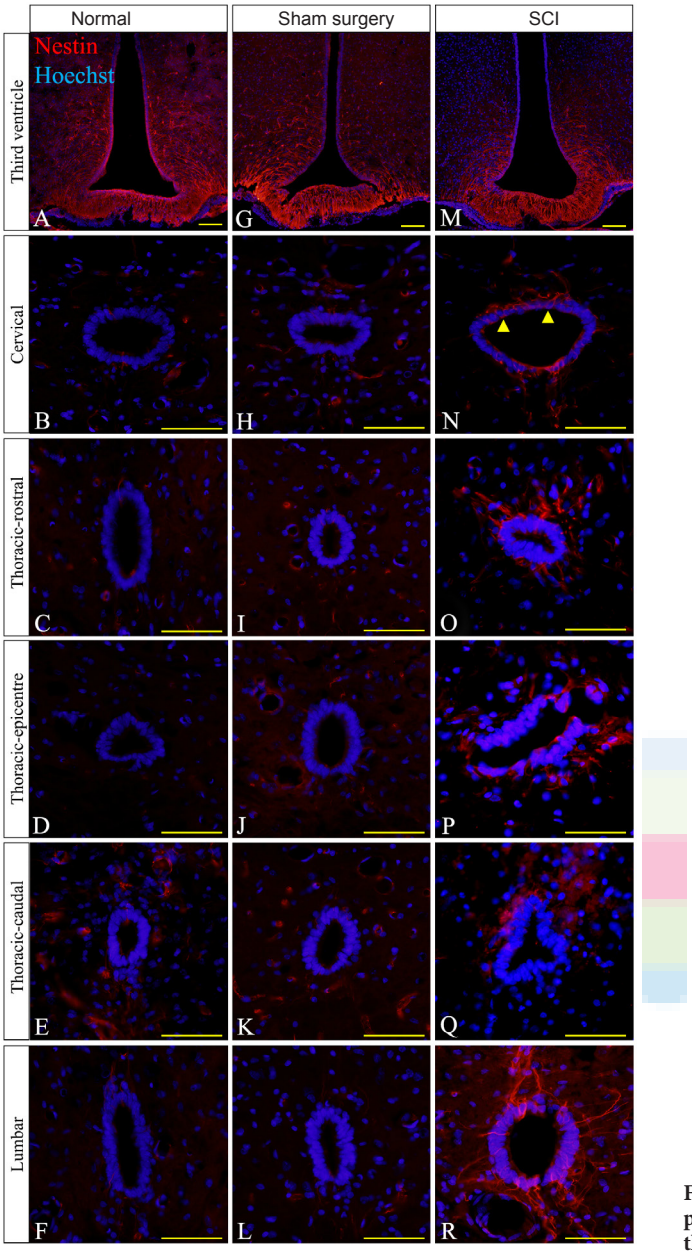

Figure 3 Immunohistochemical images of nestin reactivity in the ependymal layer in thoracic spinal cord injury (SCI) rats.
(A, G & M) Nestin reactivity (red) was highest at the third ventricle throughout the normal, sham surgery and SCI groups. (N–R) High nestin immunoreactivity was found at all regions of the spinal cord at the central canal in the SCI group compared to the normal (B–F) and sham surgery groups (H–L). For the non-injured cords, equivalent anatomical areas to the injury sites (posterior median septum and dorsal grey matter) were used instead of the lesion center and lesion edge respectively to compare nestin reactivity in each group. Hoechst 33342 solution was used as a counterstain for nuclei (blue). Scale bars: 25 μm. Arrowheads point to nestin positive cells.

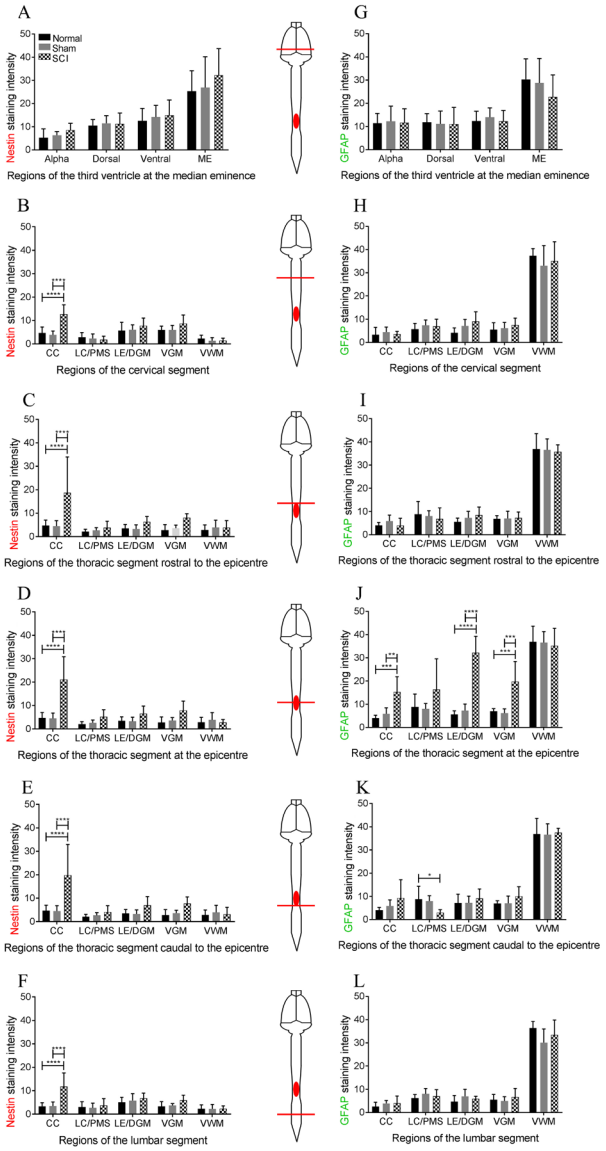

Figure 4 Graphs showing nestin and glial fibrillary acidic protein (GFAP) staining intensity of immunohistochemistry images throughout the neuroaxis in thoracic spinal cord injury rats.
(A) Mean gray scale value (GSV) of nestin staining intensity shows no significant difference at the third ventricle. (B–F) In the injury group, the mean GSV of nestin staining intensity was high at the central canal (CC) at all vertebral levels. (J) Mean GSV of GFAP staining intensity was increased in several locations at the epicenter of the lesion site. (K) Mean GSV was slightly increased in GFAP staining at the central canal 2.25 mm caudal to the epicenter. (G–I) No significant difference was found at any regions of the third ventricle, the cervical enlargement and 2.25 mm rostral to the epicenter. (L) No significant difference in GFAP staining was found at the lumbar enlargement. For the normal and sham-operated spinal cords, the posterior median septum (PMS) and dorsal grey matter (DGM) were used to compare nestin and GFAP staining intensity in the SCI group at the lesion center (LC) and lesion edge (LE) respectively. Bonferroni *post-hoc* test was used to determine significant differences in nestin and GFAP staining intensity. Error bars represent standard deviation (**$P < 0.01$, ***$P < 0.001$, ****$P < 0.0001$).

response of activated microglia to a localized injury is similar to the response of NPCs; however, microglial activation was only seen in the lumbar enlargement. Detloff et al. (2008) reported similar results in microglial activation after a thoracic SCI in rats that was also associated with below level pain (Detloff et al., 2008). They suggest that microglial activation may be due to CCL21 or Toll-like receptor 4 signaling.

This study has raised some important questions regarding the heterogeneous nature and characterization of ependymal cells and NPCs lining the central canal. Ependymal NPCs have been described quite differently by different authors including

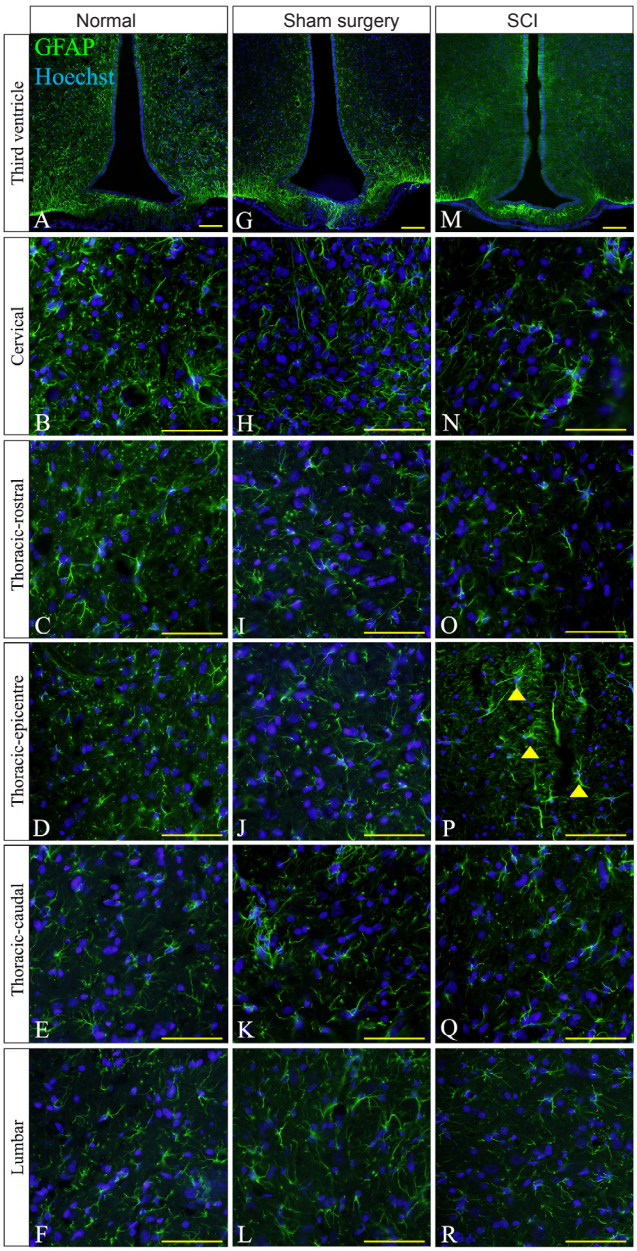

Figure 5 Immunohistochemical images of glial fibrillary acidic protein (GFAP) at the lesion edge of thoracic spinal cord injury (SCI) rats.

(A, G & M) High GFAP reactivity (green) at the third ventricle was present in the normal, sham surgery and SCI groups. (P) High GFAP immunoreactivity was only found at the epicenter of the thoracic segment of the injured spinal cord. GFAP positive cells at the epicenter showed thicker processes and higher GFAP staining intensity (arrowheads). Low GFAP immunoreactivity was detected in all spinal regions of the normal (B–F) and sham surgery (H–L) groups. Low GFAP immunoreactivity was also seen in distal regions of the SCI group (N, O, Q & R). For the non-injured spinal cords, equivalent anatomical areas to the injury sites (posterior median septum and dorsal grey matter) were used instead of the lesion center and lesion edge respectively to compare GFAP reactivity in each group. Hoechst 33342 solution was used as a counterstain for nuclei (blue). Scale bars: 25 μm.

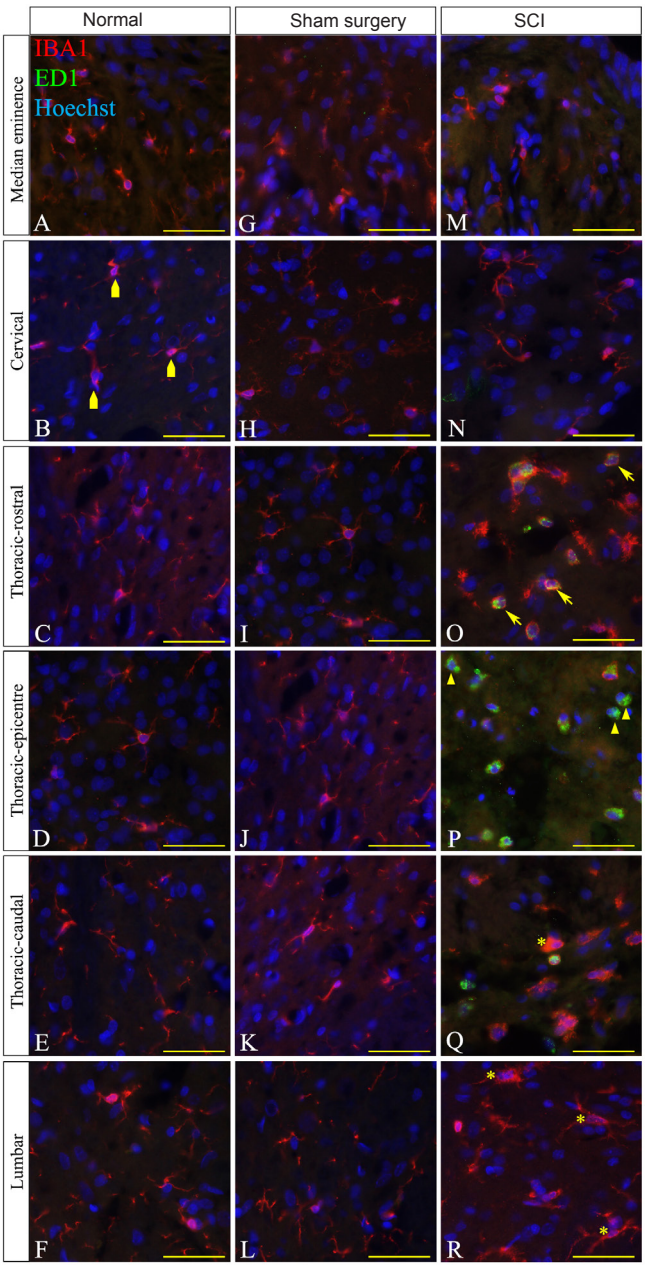

Figure 6 Immunohistochemical images of IBA1 reactivity (red) and ED1 (green) at the lesion edge in thoracic spinal cord injury (SCI) rats.

Four subsets of microglia/macrophages were identified throughout the neuroaxis; IBA1$^+$/ED1$^-$ ramified microglia (irregular pentagons), IBA1$^+$/ED1$^-$ activated microglia (asterisks), IBA1$^+$/ED1$^+$ phagocytic microglia/macrophages (arrows) and IBA1$^-$/ED1$^+$macrophages (arrowheads). IBA1$^+$/ED1$^-$ramified microglia with long and thin processes were mainly found throughout the neuroaxis of the normal and sham surgery groups (A–L). IBA1$^+$/ED1$^-$ ramified microglia were also seen in the injured neuroaxis at the median eminence, cervical enlargement and lumber enlargement (M, N, R). IBA1$^+$/ED1$^-$ activated/phagocytic microglia with either short, thick processes or amoeboid-like appearance were found at the injury site (O–Q). IBA1$^+$/ED1$^+$ phagocytic microglia/macrophages with amoeboid-like appearance were found at the injury site and highest at the epicenter (O–Q). IBA1$^-$/ED1$^+$ macrophages were found at the injury site and highest at the epicenter (O–Q). Hoechst solution was used as a counterstain for nuclei (blue). Scale bars: 25 μm.

tanycytes (Rodriguez et al., 2005), bicilliated ependymal cells (Alfaro-Cervello et al., 2012), neural stem cells (Li et al., 2006), and radial glia (Petit et al., 2011). Alfaro-Cervello and colleagues used scanning electron microscopy and immunohistochemistry to characterize ependymal cells as NPCs based on cilia counts, cell morphology, and cytoplasm content (Alfaro-Cervello et al., 2012). However, due to the diverse characteristics of the ependymal layer, it is still difficult to completely identify a NPC niche at the central canal. A detailed immunohistochemical study will be undertaken to further identify specific cell markers that differentiate these heterogeneous populations of cells and give an identification of specific function.

Overall, our study has found that early after a localized SCI, the NPC response is occurring throughout the spinal cord, the astrocyte response is localized to the level of the injury, and microglial activation extends below the lesion site. There are no changes in NPC, astrocyte, microglia, and macrophage response in the third ventricle of the brain. We suggest that NPC, and to a lesser extent, microglia are responding to signals transported through the CSF. The next step is to ascertain exactly what these signals are, and how they act on cells located distal to the injury. Several authors, including ourselves, have now suggested that spinal cord NPCs have the potential to be utilized for SCI repair (Obermair et al., 2008; Gregoire et al., 2015; Stenudd et al., 2015; Mao et al., 2016b). The findings of the current study should be considered when deciding how to manipulate specific cell populations. If spinal cord ependymal cells are reacting to a localized injury throughout the spinal cord, care should be taken when attempting to manipulate these cells *in vivo*. It is unknown at this stage whether over stimulation or increased up-regulation of NPC by a therapeutic agent will lead to abnormal or extensive cell proliferation in areas where it is not expected or wanted.

Acknowledgments: *To note intellectual, technical or other assistance that does not warrant authorship. We would like to acknowledge the staff from the Ernst facility for their assistance in animal care.*
Author contributions: *TN was responsible for tissue processing. YM was in charge of surgical procedure and tissue processing, and contributed to preparation of discussion section. TS participated in tissue processing and contributed to preparation of results and discussion. CAG designed the study and contributed to preparation of introduction and discussion sections. All authors approved the final version of this paper.*
Conflicts of interest: *None declared.*
Research ethics: *All surgical procedures were conducted strictly under the guidelines described by the National Health and Medical Research Council code of conduct for animals and the institutional Animal Care and Ethics Committee approved this study (UTS ACEC13-0069).*
Data sharing statement: *Datasets analyzed during the current study are available from the corresponding author on reasonable request.*
Plagiarism check: *Checked twice by iThenticate.*
Peer review: *Externally peer reviewed.*

References

Ahadi R, Khodagholi F, Daneshi A, Vafaei A, Mafi AA, Jorjani M (2015) Diagnostic value of serum levels of GFAP, pNF-H, and NSE compared with clinical findings in severity assessment of human traumatic spinal cord injury. Spine 40:E823-830.

Alfaro-Cervello C, Soriano-Navarro M, Mirzadeh Z, Alvarez-Buylla A, Garcia-Verdugo JM (2012) Biciliated ependymal cell proliferation contributes to spinal cord growth. J Comp Neurol 520:3528-3552.

Ayoub AE, Salm AK (2003) Increased morphological diversity of microglia in the activated hypothalamic supraoptic nucleus. J Neurosci 23:7759-7766.

Barnabe-Heider F, Goritz C, Sabelstrom H, Takebayashi H, Pfrieger FW, Meletis K, Frisen J (2010) Origin of new glial cells in intact and injured adult spinal cord. Cell Stem Cell 7:470-482.

Basso DM, Beattie MS, Bresnahan JC, Anderson DK, Faden AI, Gruner JA, Holford TR, Hsu CY, Noble LJ, Nockels R, Perot PL, Salzman SK, Young W (1996) MASCIS evaluation of open field locomotor scores: effects of experience and teamwork on reliability. Multicenter Animal Spinal Cord Injury Study. J Neurotrauma 13:343-359.

Blasko J, Martoncikova M, Lievajova K, Saganova K, Korimova A, Racekova E (2012) Regional differences of proliferation activity in the spinal cord ependyma of adult rats. Cent Eur J Biol 7:397-403.

Cawsey T, Duflou J, Weickert CS, Gorrie CA (2015) Nestin-positive ependymal cells are increased in the human spinal cord after traumatic central nervous system injury. J Neurotrauma 32:1393-1402.

Chan WM, Mohammed Y, Lee I, Pearse DD (2013) Effect of gender on recovery after spinal cord injury. Transl Stroke Res 4:447-461.

Cizkova D, Nagyova M, Slovinska L, Novotna I, Radonak J, Cizek M, Mechirova E, Tomori Z, Hlucilova J, Motlik J, Sulla I Jr, Vanicky I (2009) Response of ependymal progenitors to spinal cord injury or enhanced physical activity in adult rat. Cell Mol Neurobiol 29:999-1013.

Decimo I, Bifari F, Rodriguez FJ, Malpeli G, Dolci S, Lavarini V, Pretto S, Vasquez S, Sciancalepore M, Montalbano A, Berton V, Krampera M, Fumagalli G (2011) Nestin- and doublecortin-positive cells reside in adult spinal cord meninges and participate in injury-induced parenchymal reaction. Stem Cells 29:2062-2076.

Detloff MR, Fisher LC, McGaughy V, Longbrake EE, Popovich PG, Basso D (2008) Remote activation of microglia and pro-inflammatory cytokines predict the onset and severity of below-level neuropathic pain after spinal cord injury in rats. Exp Neurol 212:337-347.

do Carmo Cunha J, de Freitas Azevedo Levy B, de Luca BA, de Andrade MS, Gomide VC, Chadi G (2007) Responses of reactive astrocytes containing S100beta protein and fibroblast growth factor-2 in the border and in the adjacent preserved tissue after a contusion injury of the spinal cord in rats: implications for wound repair and neuroregeneration. Wound Repair Regen 15:134-146.

Eng LF, Ghirnikar RS (1994) GFAP and astrogliosis. Brain Pathol 4:229-237.

Eriksson PS, Perfilieva E, Bjork-Eriksson T, Alborn AM, Nordborg C, Peterson DA, Gage FH (1998) Neurogenesis in the adult human hippocampus. Nat Med 4:1313-1317.

Fitch MT, Silver J (2008) CNS injury, glial scars, and inflammation: Inhibitory extracellular matrices and regeneration failure. Exp Neurol 209:294-301.

Fleming JC, Norenberg MD, Ramsay DA, Dekaban GA, Marcillo AE, Saenz AD, Pasquale-Styles M, Dietrich WD, Weaver LC (2006) The cellular inflammatory response in human spinal cords after injury. Brain 129:3249-3269.

Foret A, Quertainmont R, Botman O, Bouhy D, Amabili P, Brook G, Schoenen J, Franzen R (2010) Stem cells in the adult rat spinal cord: plasticity after injury and treadmill training exercise. J Neurochem 112:762-772.

Gaudet AD, Popovich PG (2014) Extracellular matrix regulation of inflammation in the healthy and injured spinal cord. Exp Neurol 0:24-34.

Goodman T, Hajihosseini MK (2015) Hypothalamic tanycytes—masters and servants of metabolic, neuroendocrine, and neurogenic functions. Front Neurosci 9:387.

Gorrie CA, Hayward I, Cameron N, Kailainathan G, Nandapalan N, Sutharsan R, Wang J, Mackay-Sim A, Waite PM (2010) Effects of human OEC-derived cell transplants in rodent spinal cord contusion injury. Brain Res 1337:8-20.

Greenhalgh AD, David S (2014) Differences in the phagocytic response of microglia and peripheral macrophages after spinal cord injury and its effects on cell death. J Neurosci 34:6316-6322.

Gregoire CA, Goldenstein BL, Floriddia EM, Barnabe-Heider F, Fernandes KJ (2015) Endogenous neural stem cell responses to stroke and spinal cord injury. Glia 63:1469-1482.

Guo Y, Liu S, Zhang X, Wang L, Zhang X, Hao A, Han A, Yang J (2014) Sox11 promotes endogenous neurogenesis and locomotor recovery in mice spinal cord injury. Biochem Biophys Res Commun 446:830-835.
Gwak YS, Hulsebosch CE (2009) Remote astrocytic and microglial activation modulate neuronal hyperexcitability and below-level neuropathic pain after spinal injury in rat. Neuroscience 161:895-903.
Haan N, Goodman T, Najdi-Samiei A, Stratford CM, Rice R, El Agha E, Bellusci S, Hajihosseini MK (2013) Fgf10-expressing tanycytes add new neurons to the appetite/energy-balance regulating centers of the postnatal and adult hypothalamus. J Neurosci 33:6170-6180.
Hamilton LK, Truong MK, Bednarczyk MR, Aumont A, Fernandes KJ (2009) Cellular organization of the central canal ependymal zone, a niche of latent neural stem cells in the adult mammalian spinal cord. Neuroscience 164:1044-1056.
Karimi-Abdolrezaee S, Billakanti R (2012) Reactive astrogliosis after spinal cord injury-beneficial and detrimental effects. Mol Neurobiol 46:251-264.
Ke Y, Chi L, Xu R, Luo C, Liu R (2006) Early response of endogenous adult neural progenitor cells to acute spinal cord injury in mice. Stem Cells 24:1011-1019.
Kwon BK, Streijger F, Fallah N, Noonan VK, Belanger LM, Ritchie L, Paquette SJ, Ailon T, Boyd MC, Street J, Fisher CG, Dvorak MF (2017) Cerebrospinal fluid biomarkers to stratify injury severity and predict outcome in human traumatic spinal cord injury. J Neurotrauma 34:567-580.
Kwon BK, Stammers AM, Belanger LM, Bernardo A, Chan D, Bishop CM, Slobogean GP, Zhang H, Umedaly H, Giffin M, Street J, Boyd MC, Paquette SJ, Fisher CG, Dvorak MF (2010) Cerebrospinal fluid inflammatory cytokines and biomarkers of injury severity in acute human spinal cord injury. J Neurotrauma 27:669-682.
Lendahl U, Zimmerman LB, McKay RD (1990) CNS stem cells express a new class of intermediate filament protein. Cell 60:585-595.
Li W, Cai WQ, Li CR (2006) Repair of spinal cord injury by neural stem cells modified with BDNF gene in rats. Neurosci Bull 22:34-40.
Liu D, Xu GY, Pan E, McAdoo DJ (1999) Neurotoxicity of glutamate at the concentration released upon spinal cord injury. Neuroscience 93:1383-1389.
Mao Y, Mathews K, Gorrie CA (2016a) Temporal response of endogenous neural progenitor cells following injury to the adult rat spinal cord. Front Cell Neurosci 10:58.
Mao Y, Nguyen T, Sutherland T, Gorrie CA (2016b) Endogenous neural progenitor cells in the repair of the injured spinal cord. Neural Regen Res 11:1075-1076.
Martens DJ, Seaberg RM, van der Kooy D (2002) In vivo infusions of exogenous growth factors into the fourth ventricle of the adult mouse brain increase the proliferation of neural progenitors around the fourth ventricle and the central canal of the spinal cord. Eur J Neurosci 16:1045-1057.
Meletis K, Barnabé-Heider F, Carlén M, Evergren E, Tomilin N, Shupliakov O, Frisén J (2008) Spinal cord injury reveals multilineage differentiation of ependymal cells. PLoS Biol 6:e182.
Migaud M, Batailler M, Segura S, Duittoz A, Franceschini I, Pillon D (2010) Emerging new sites for adult neurogenesis in the mammalian brain: a comparative study between the hypothalamus and the classical neurogenic zones. Eur J Neurosci 32:2042-2052.
Ming GL, Song H (2005) Adult neurogenesis in the mammalian central nervous system. Annu Rev Neurosci 28:223-250.
Mokry J, Ehrmann J, Karbanova J, Cizkova D, Soukup T, Suchanek J, Filip S, Kolar Z (2008) Expression of intermediate filament nestin in blood vessels of neural and non-neural tissues. Acta Medica (Hradec Kralove) 51:173-179.
Morgenstern DA, Asher RA, Fawcett JW (2002) Chondroitin sulphate proteoglycans in the CNS injury response. Prog Brain Res 137:313-332.
Mortazavi MM, Verma K, Harmon OA, Griessenauer CJ, Adeeb N, Theodore N, Tubbs RS (2015) The microanatomy of spinal cord injury: a review. Clin Anat 28:27-36.
Neumann H, Kotter MR, Franklin RJM (2009) Debris clearance by microglia: an essential link between degeneration and regeneration. Brain 132:288-295.
Obermair FJ, Schroter A, Thallmair M (2008) Endogenous neural progenitor cells as therapeutic target after spinal cord injury. Physiology (Bethesda) 23:296-304.
Ohtake Y, Smith GM, Li S (2016) Reactive astrocyte scar and axon regeneration: suppressor or facilitator? Neural Regen Res 11:1050-1051.
Paxinos G. WC (1996) The Rat Brain in Sterotaxic Coordinate, Compact Third Edition Edition. New York: Academic Press.
Petit A, Sanders AD, Kennedy TE, Tetzlaff W, Glattfelder KJ, Dalley RA, Puchalski RB, Jones AR, Roskams AJ (2011) Adult spinal cord radial glia display a unique progenitor phenotype. PLoS One 6:e24538.
Pineau I, Lacroix S (2007) Proinflammatory cytokine synthesis in the injured mouse spinal cord: multiphasic expression pattern and identification of the cell types involved. J Comp Neurol 500:267-285.
Prieto M, Chauvet N, Alonso G (2000) Tanycytes transplanted into the adult rat spinal cord support the regeneration of lesioned axons. Exp Neurol 161:27-37.
Rafols JA, Goshgarian HG (1985) Spinal tanycytes in the adult rat: a correlative Golgi gold-toning study. Anat Rec 211:75-86.
Rodriguez EM, Blazquez JL, Pastor FE, Pelaez B, Pena P, Peruzzo B, Amat P (2005) Hypothalamic tanycytes: a key component of brain-endocrine interaction. Int Rev Cytol 247:89-164.
Schwindt TT, Motta FL, Gabriela FB, Cristina GM, Guimaraes AO, Calcagnotto ME, Pesquero JB, Mello LE (2009) Effects of FGF-2 and EGF removal on the differentiation of mouse neural precursor cells. An Acad Bras Cienc 81:443-452.
Shibuya S, Miyamoto O, Auer RN, Itano T, Mori S, Norimatsu H (2002) Embryonic intermediate filament, nestin, expression following traumatic spinal cord injury in adult rats. Neuroscience 114:905-916.
Shihabuddin LS (2008) Adult rodent spinal cord-derived neural stem cells: isolation and characterization. Methods Mol Biol 438:55-66.
Stammers AT, Liu J, Kwon BK (2012) Expression of inflammatory cytokines following acute spinal cord injury in a rodent model. J Neurosci Res 90:782-790.
Stenudd M, Sabelstrom H, Frisen J (2015) Role of endogenous neural stem cells in spinal cord injury and repair. JAMA Neurol 72:235-237.
Streit WJ, Mrak RE, Griffin WS (2004) Microglia and neuroinflammation: a pathological perspective. J Neuroinflammation 1:14.
Sun D, Jakobs TC (2012) Structural remodeling of astrocytes in the injured CNS. Neuroscientist 18:567-588.
Sutherland TC, Mathews KJ, Mao Y, Nguyen T, Gorrie CA (2017) Differences in the cellular response to acute spinal cord injury between developing and mature rats highlights the potential significance of the inflammatory response. Front Cell Neurosci 10:310.
Takahashi M, Arai Y, Kurosawa H, Sueyoshi N, Shirai S (2003) Ependymal cell reactions in spinal cord segments after compression injury in adult rat. J Neuropathol Exp Neurol 62:185-194.
Taupin P, Gage FH (2002) Adult neurogenesis and neural stem cells of the central nervous system in mammals. J Neurosci Res 69:745-749.
Tureyen K, Vemuganti R, Bowen KK, Sailor KA, Dempsey RJ (2005) EGF and FGF-2 infusion increases post-ischemic neural progenitor cell proliferation in the adult rat brain. Neurosurgery 57:1254-1263; discussion 1254-1263.
Weiss S, Dunne C, Hewson J, Wohl C, Wheatley M, Peterson AC, Reynolds BA (1996) Multipotent CNS stem cells are present in the adult mammalian spinal cord and ventricular neuroaxis. J Neurosci 16:7599-7609.
Xu Y, Tamamaki N, Noda T, Kimura K, Itokazu Y, Matsumoto N, Dezawa M, Ide C (2005) Neurogenesis in the ependymal layer of the adult rat 3rd ventricle. Exp Neurol 192:251-264.
Zhou X, He X, Ren Y (2014) Function of microglia and macrophages in secondary damage after spinal cord injury. Neural Regen Res 9:1787-1795.

Copyedited by Li CH, Song LP, Zhao M

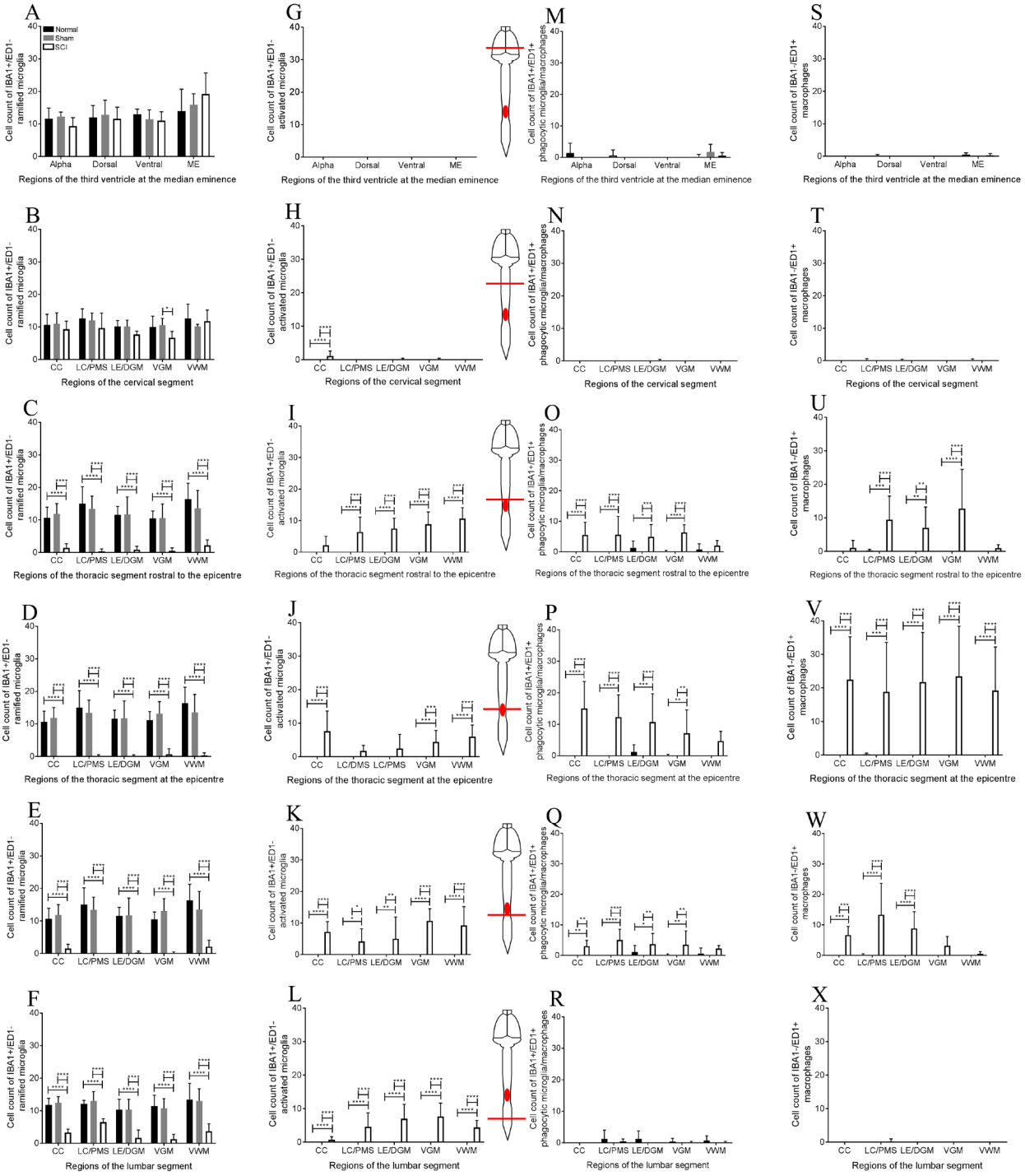

Figure 7 Cell counts of IBA1$^+$/ED1$^-$ ramified microglia, IBA1$^+$/ED1$^-$ activated/phagocytic microglia, IBA1$^+$/ED1$^+$ phagocytic microglia/macrophages and IBA1$^-$/ED1$^+$ macrophages.

(A, B) IBA1$^+$/ED1$^-$ ramified microglia cell counts at the third ventricle and the cervical enlargement. (C–F) Significant difference was found in IBA1$^+$/ED1$^-$ ramified microglia cell counts at all regions of the injured spinal segments compared to the normal and sham surgery groups. (G) No IBA1$^+$/ED1$^-$ activated microglia were found at the third ventricle of the neuroaxis. (H–L) Significant difference in IBA1$^+$/ED1$^-$ activated microglia was found throughout the injured spinal segments in the SCI group compared to the normal and sham surgery groups. (M, N, R) No significant difference in IBA1$^+$/ED1$^+$ phagocytic microglia/macrophages was found at the third ventricle, cervical enlargement and lumbar enlargement. (O–Q) IBA1$^+$/ED1$^+$ phagocytic microglia/macrophages cell counts were significantly increased at the lesion site in the SCI group compared to the normal and sham surgery groups. (S, T, X) No significant difference in IBA1$^-$/ED1$^+$ macrophage cell counts was found at the third ventricle, cervical enlargement and lumbar enlargement. (U–W) Cell counts of IBA1$^-$/ED1$^+$ macrophages were significantly higher at the lesion site in the SCI group compared to the normal and sham surgery groups. For the normal and sham-operated spinal cords, the posterior median septum (PMS) and dorsal grey matter (DGM) were used to compare IBA1 and ED1 staining intensity in the SCI group at the lesion center (LC) and lesion edge (LE) respectively. Bonferroni *post-hoc* test was used to determine significant differences in IBA1 and ED1 cell counts. Error bars represent standard deviation (*P < 0.05, **P < 0.01, ***P < 0.001, ****P < 0.0001).